

# Caged Glutathione – Triggering Protein Interaction by Light\*\*

Volker Gatterdam, Tatjana Stoess, Clara Menge, Alexander Heckel,\* and Robert Tampé\*

The pseudotripeptide glutathione (GSH), consisting of glutamate, cysteine, and glycine, is essential for the regulation of the redox environment and detoxification in eukaryotic cells.<sup>[1]</sup> The ratio of reduced GSH and oxidized GSSG controls the redox potential in cellular compartments.<sup>[2]</sup> Furthermore, GSH acts as an important redox scavenger of reactive oxygen species (ROS) in aging and host–pathogen interactions, causing oxidative stress involved in many diseases, such as Alzheimer's, Parkinson's, liver disease, sickle-cell anemia, parasitic diseases,<sup>[3]</sup> AIDS, cancer,<sup>[4]</sup> cardiac diseases, and diabetes.<sup>[5]</sup> Furthermore, the nucleophilic thiol of GSH is used by glutathione S-transferase (GST) enzymes to covalently bind xenobiotics, such as drugs, toxins, or ROS.<sup>[6]</sup> GSH conjugates can then be secreted by the glutathione S-conjugate transporters for detoxification.<sup>[7]</sup> GSH recognition by GST is widely exploited in life science, for example, protein purification,<sup>[8]</sup> high-throughput protein–protein interaction screens,<sup>[9]</sup> or protein immobilization.<sup>[10]</sup>

Herein, we describe an approach to trigger the generic GSH–protein interaction by light. An optimal compatibility with cells or even animals is given by the usage of wavelengths in the visible spectrum, which do not harm the target. Light can be regulated very precisely, thus making a spatial, temporal, and dosage control possible. In recent years, many photoactivatable approaches have been realized.<sup>[11]</sup> Important examples are caged biotin,<sup>[12]</sup> caged O<sup>6</sup>-benzylguanine,<sup>[13]</sup> and photoactivatable trisNTA,<sup>[14]</sup> but also light-controlled applications<sup>[15]</sup> such as peptide synthesis,<sup>[16]</sup> gene regulation,<sup>[17]</sup> and structured cell adhesion<sup>[18]</sup> are emerging fields.

Photoactivatable glutathione was designed by modification of the amino and carboxyl groups that strongly impact the recognition by GST and a number of other GSH-binding proteins. The photoactivatable nitrophenylpropyl (NPP) protection group was chosen.<sup>[19]</sup> Based on the X-ray structure of GST with bound GSH, the amino and carboxyl moiety of the  $\gamma$ -L-glutamyl residue as well as the carboxyl group of the glycine were identified as putative interaction sites<sup>[20]</sup> that are available for chemical modification (Figure 1).

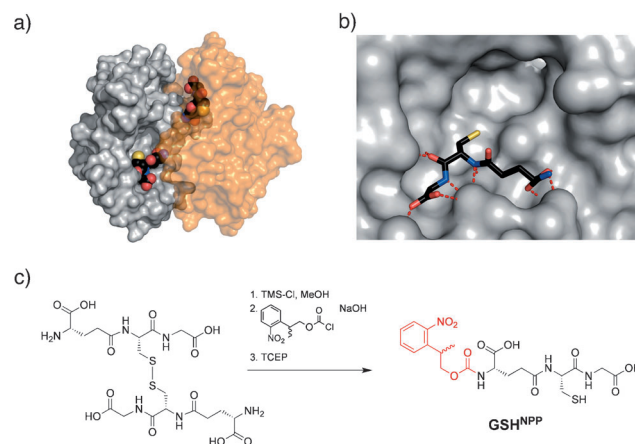


**Figure 1.** a) X-ray structure of the human glutathione S-transferase M2-2 with bound GSH (PDB: 1XW5).<sup>[21]</sup> b) The GSH binding pockets of the homodimer are in the gap between both monomers. Dotted red lines illustrate the interaction network between GST and GSH. The SH function of the cysteine is freely accessible. c) Synthesis and structure of photoactivatable GSH derivatives **GSH<sup>NPP</sup>**. TMS-Cl = trimethylsilyl chloride; TCEP = tris(2-carboxyethyl)phosphine hydrochloride.

We synthesized a doubly and a singly caged GSH, **GSH<sup>NPP2</sup>** and **GSH<sup>NPP</sup>**, respectively (see the Supporting Information). The former displayed very low solubility in aqueous solution, and in particular after coupling to fluorophores. Therefore, **GSH<sup>NPP2</sup>** was applied only in protein interaction studies at interfaces. Protection at the C-terminus of glycine was also realized but is not described herein. The sulfhydryl group of GSH was used for covalent modification with various fluorophores and functionalization of interfaces. These modifications should not interfere with the GST binding, because they are used for coupling to xenobiotics in the cellular environment. The expression of GST fusion proteins is well-established<sup>[8]</sup> and allows almost any protein of interest to be fused to GST.

We first investigated the specificity and rate of the deprotection reaction of **GSH<sup>NPP</sup>** by reverse-phase HPLC. The photoreaction was triggered at 366 nm using an LED (140 mW cm<sup>-2</sup>). For sensitive detection, the fluorophore ATTO565 (as maleimide derivative) was covalently coupled

[\*] V. Gatterdam,<sup>[†]</sup> Prof. Dr. R. Tampé  
Institute of Biochemistry, Biocenter  
Cluster of Excellence Frankfurt (CEF)  
Goethe University Frankfurt  
Max-von-Laue-Strasse 9, 60438 Frankfurt am Main (Germany)  
E-mail: tampe@em.uni-frankfurt.de  
Homepage: <http://www.biochem.uni-frankfurt.de>  
T. Stoess,<sup>[†]</sup> C. Menge, Prof. Dr. A. Heckel  
Frankfurt Institute for Molecular Life Sciences  
Cluster of Excellence Frankfurt (CEF)  
Goethe University Frankfurt  
Max-von-Laue-Strasse 9, 60438 Frankfurt am Main (Germany)  
E-mail: heckel@uni-frankfurt.de

[†] Both authors contributed equally to this work.

[\*\*] This work was supported by the DFG through the Cluster of Excellence Macromolecular Complexes (EXC 115) and by the Goethe University Frankfurt. A generous donation of silyl protecting group precursors by the Wacker Company and the GST-eGFP vector by T. Nuutinen and Prof. J. Syväoja (University of East Finland) is gratefully acknowledged.

Supporting information for this article is available on the WWW under <http://dx.doi.org/10.1002/anie.201108073>.

to the cysteine of **GSH<sup>NPP</sup>**. This fluorescent **GSH<sup>NPP</sup>** (10 nmol in TBS buffer) was illuminated for different periods. After 60 s, no starting material and only minute amounts of side products were detected (Figure 2). The deprotection follows

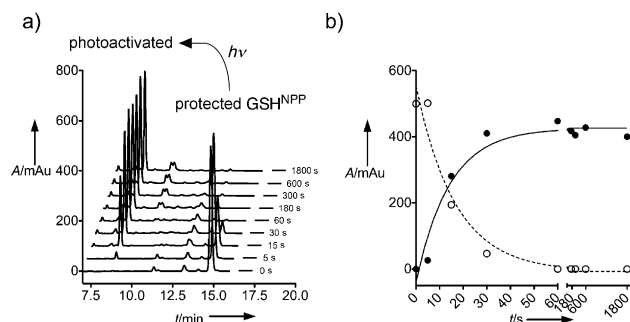


**Figure 2.** Time-dependent photoactivation of ATTO565-labeled **GSH<sup>NPP</sup>** monitored by reverse-phase HPLC. a) Time series of the deprotection reaction followed at 254 nm. Caged and uncaged **GSH<sup>NPP</sup>** elute at 15.0 and 8.5 min, respectively. The identity of the photoproduct was confirmed by ESI-MS. b) The starting material (○) is consumed at a rate of  $(0.060 \pm 0.013) \text{ s}^{-1}$  and the rate of formation of the uncaged product (●) is  $(0.071 \pm 0.016) \text{ s}^{-1}$ .

a monoexponential decay in combination with a monoexponential growth of the product. In the range of error, the rate constant for the consumption of the starting material ( $(0.060 \pm 0.013) \text{ s}^{-1}$ ,  $\tau_{1/2} = (11.5 \pm 3.1) \text{ s}$ ), and formation of the product ( $(0.071 \pm 0.016) \text{ s}^{-1}$ ,  $\tau_{1/2} = (9.8 \pm 2.8) \text{ s}$ ) are identical, indicating a one-step deprotection without rate-limiting intermediates. We also examined the long-term stability by 30 minute illumination. No major photo-damage of the uncaged product or bleaching of the fluorophore was observed. In conclusion, we demonstrate a fast, one-step photoactivation of **GSH<sup>NPP</sup>** without intermediate compounds.

To follow the GSH-GST interaction in real time, we established a Förster resonance energy transfer (FRET) assay using GST C-terminally fused to enhanced green fluorescent protein (eGFP) and ATTO565-labeled **GSH<sup>NPP</sup>** as the donor-acceptor pair. GST-eGFP (10 nm in TBS buffer) was incubated with caged and uncaged (ATTO-labeled) **GSH<sup>NPP</sup>**, respectively. Titration with labeled **GSH<sup>NPP</sup>** showed no significant FRET (see the Supporting Information). However, illumination of labeled **GSH<sup>NPP</sup>** leads to a significant FRET demonstrated by an increase and decrease of the acceptor and donor fluorescence, respectively (Figure 3a,b). The  $K_D$  of non-illuminated ATTO565-labeled **GSH<sup>NPP</sup>** was  $(53 \pm 2) \text{ nM}$ , which indicates a higher affinity than GSH.<sup>[22]</sup> Results were confirmed by validation of the acceptor fluorescence, which yielded in a similar value of  $K_D$ .<sup>[23]</sup> The light-triggered GSH-GST interaction was followed in real time by FRET. GST-eGFP (10 nm) and ATTO565-labeled **GSH<sup>NPP</sup>** (500 nm) were illuminated at 366 nm. After photoactivation, an increase and decrease of acceptor and donor fluorescence, respectively, was detected (Figure 3c). Notably, the reaction rate is limited by the diffusion of **GSH<sup>NPP</sup>** through the very small illumination spot in the cuvette (Figure 3d) and therefore not comparable to the true rate of reaction.

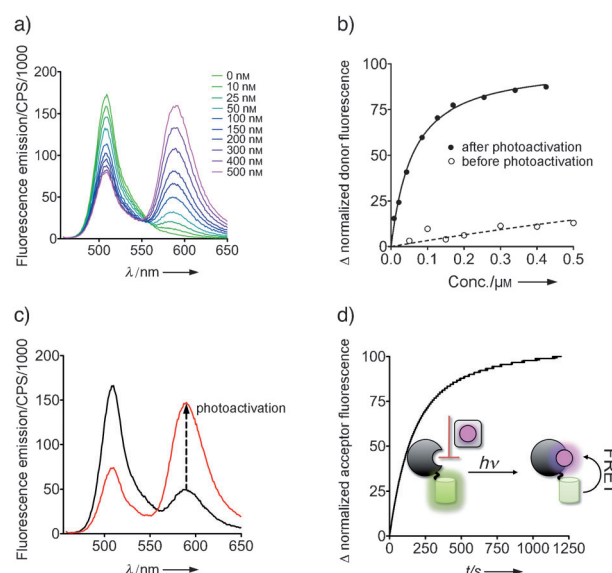


**Figure 3.** Light-triggered GSH-GST interaction detected using FRET. a) Complex formation with GSH and GST was followed using GST-eGFP (10 nm) as FRET donor. Increasing concentrations of ATTO565-labeled **GSH<sup>NPP</sup>** as FRET acceptor were added before (see the Supporting Information) and after photoactivation. The donor was excited at 450 nm. Photoactivation leads to a dramatic decrease of donor fluorescence and increase of the acceptor fluorescence, demonstrating complex formation. b) The donor fluorescence was corrected towards dilution and inner filter effects with appropriate experiments. The inverted and normalized change in donor fluorescence at 511 nm is plotted against the concentration of FRET acceptor and fitted with Equation (1) (see the Supporting Information), yielding a  $K_D$  of  $(53 \pm 2) \text{ nM}$  after photoactivation (●). A very low affinity interaction was observed before photoactivation (○). c) An extensive spectral change was observed before (black) and after photoactivation (at 366 nm, red) of a mixture of GST-eGFP (10 nm) and labeled **GSH<sup>NPP</sup>** (500 nm). d) Interaction of GST-eGFP (10 nm) and labeled **GSH<sup>NPP</sup>** (500 nm) followed by FRET in real time. The acceptor fluorescence at 592 nm was recorded by excitation of the donor at 366 nm, which also triggers the photoactivation process. CPS = counts per second.

We next studied the in situ assembly of GST fusion proteins on **GSH<sup>NPP</sup>**- and **GSH<sup>NPP2</sup>**-functionalized surfaces by light. Light-directed protein organization was performed by the use of a quartz glass mask covered with a chrome pattern of different grid sizes. The mask was placed on top of the **GSH<sup>NPP</sup>**- or **GSH<sup>NPP2</sup>**-functionalized glass slides and illuminated at 366 nm (Xe/Hg lamp, 200 W) for 3 minutes. During structured illumination, the functionalized interfaces were incubated with GST-eGFP (500 nm). Confocal laser scanning microscopy (CLSM) was used to monitor the process of photoactivation and assembly. Defined structures of GST-eGFP at the photopattern areas could be observed (Figure 4a). Superb contrast over large areas reflects the high specificity of the photoactivation of **GSH<sup>NPP</sup>**. However, owing to the hydrophobicity of doubly caged **GSH<sup>NPP2</sup>**, a dramatic increase of unspecific protein binding was detected at the **GSH<sup>NPP2</sup>**-functionalized interfaces (see the Supporting Information). Despite the fast on and off binding kinetics, the protein patterns at photoactivated **GSH<sup>NPP</sup>** interfaces were stable over several days and could be reused for further

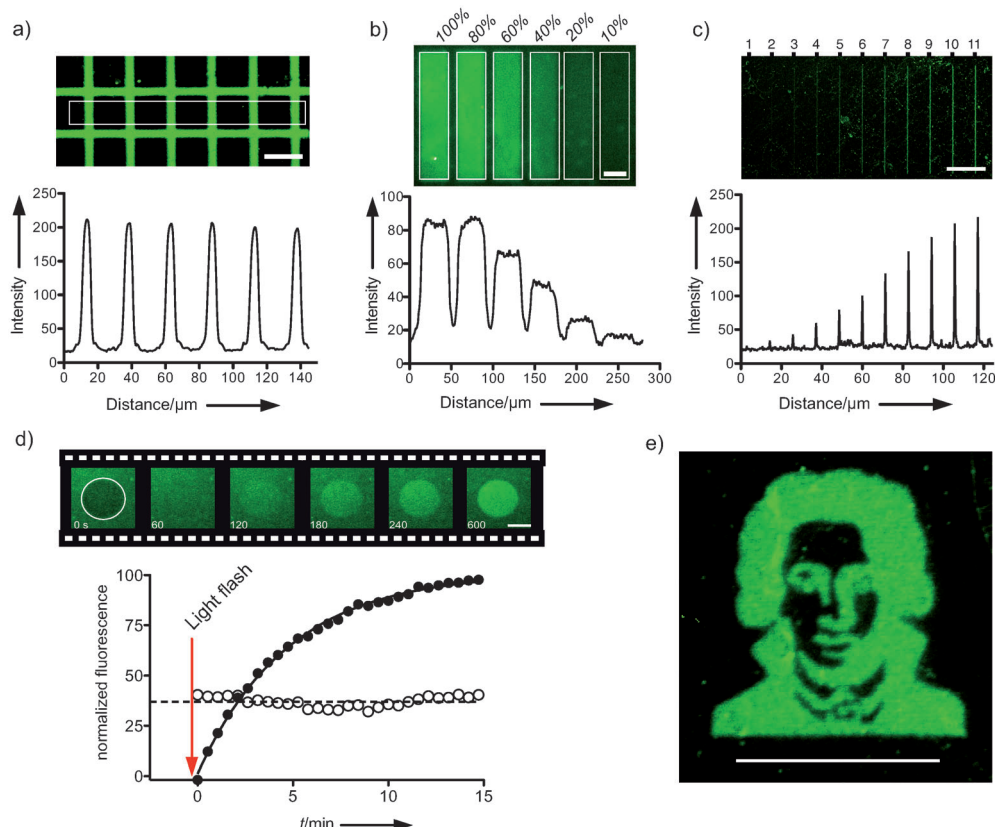


**Figure 4.** In situ assembly of GST fusion proteins triggered by light. a) Protein-resistant PEGylated interfaces are functionalized with **GSH<sup>NPP</sup>** and illuminated at 366 nm by mask lithography. Binding of GST-eGFP (500 nm) was analyzed after washing with TBS buffer by confocal laser scanning microscopy. A 488 nm argon laser (10% max. power, 30 mW) was used for excitation. A patterning with well-defined edges and high contrast was observed. An intensity profile was taken across the indicated area. b) Different lateral densities of GST fusion proteins were generated by in situ patterning using increased illumination power of the 405 nm UV diode laser (100% max. power, 20 mW). The structures were visualized with a 488 nm argon laser. c) To determine the spatial resolution, a single line was written with different iterations (41 ms for one scan,  $0.29 \mu\text{m} \times 58.0 \mu\text{m}$ ). The first protein pattern could already be seen after two iterations (82 ms). Increasing the number of iterations leads to a blurring of the structure owing to the Gaussian illumination distribution. d) In situ protein assembly followed in real time. A **GSH<sup>NPP</sup>**-functionalized protein-resistant PEGylated interface was illuminated with a 405 nm laser in the highlighted spot for less than 10 s. Monitoring with a 488 nm laser revealed the real-time binding kinetics of GST-eGFP (500 nm in TBS buffer). Analysis with a monoexponential growth of GST-eGFP fluorescence (●) revealed an association rate constant of  $(0.21 \pm 0.01) \text{ min}^{-1}$  ( $\tau_{1/2} = 3.3 \pm 0.1 \text{ min}$ ). ○ represent the fluorescence of GST-eGFP (500 nm) present in solution. e) Free design of protein arrays using the 405 nm laser with one iteration only (<1 min). The white bar indicates  $20 \mu\text{m}$  in all images.

experiments. It was possible to dissociate the protein pattern by incubation with release buffer (10 mM glycine, pH 2.0) in less than 10 seconds. After equilibration of the recovered slides in TBS buffer, an identical pattern of GST-eGFP could be restored. Apart from mask lithography, in situ patterning with a scanning laser was also conducted. Freely designed regions were illuminated with the 405 nm diode laser and the assembly of GST-eGFP was followed by CLSM ( $\lambda_{\text{ex/em}} = 488/520 \text{ nm}$ ). Different protein densities could be achieved by varying the illumination power (Figure 4b).

To investigate the spatial resolution, the interface was illuminated by a point laser source. The numerical aperture of the objective lens and the laser wavelength determine the focal volume. Diffraction-limited lines ( $0.29 \mu\text{m}$  thick and  $58 \mu\text{m}$  in length) were scanned by the 405 nm laser in 41 ms.

Patterns can already be detected after two iterations (82 ms). The observed lines have a full width at half maximum (FWHM) of 500 nm (Figure 4c). Even faster writing times can be achieved by downsizing the structures. Higher iteration numbers lead to saturation and blurring of the structure.

We then followed the binding of GST-eGFP (500 nm) in real time. Activation with the 405 nm laser was performed by a single iteration (light flash) followed by immediate monitoring of the GST-eGFP fluorescence (Figure 4d). The exponential binding kinetics revealed a  $k_{\text{on}}$  value of  $0.2 \text{ min}^{-1}$ . Thus, sequential writing and parallel readout of complex structures were realized. We finally used the 405 nm laser to assemble GST fusion proteins in freely designed patterns (Figure 4e). By use of several GST fusion proteins, a multiprotein surface<sup>[10]</sup> with defined areas can be generated under light control. Therefore, protein complexes and the GSH-GST interaction networks<sup>[24]</sup> can be controlled by light.

In conclusion, we introduced a new photoactivatable capturing tag based on the GST-GSH interaction.

The compound **GSH<sup>NPP</sup>** can be functionalized in a versatile way on the free cysteine without affecting the GST interaction. Functionalization with bulky fluorophores and covalent immobilization was demonstrated without interfering with the complex formation. The deprotection with light is very fast and complete in less than a millisecond to second range. The system has a very good temporal resolution. This is an advantage in terms of photo damage in vitro and in vivo. Furthermore, a good spatial resolution was achieved by the use of a CLSM, allowing the illumination and reading of  $0.5 \mu\text{m}$  thick lines, which is limited by the optical resolution.

Received: November 16, 2011

Published online: March 5, 2012

**Keywords:** glutathione S-transferase · light-triggered chemical biology · photoactivatable compounds · photoactivation · protein immobilization

- [1] J. D. Hayes, L. I. McLellan, *Free Radical Res.* **1999**, *31*, 273–300.
- [2] a) H. F. Gilbert, *Methods Enzymol.* **1984**, *107*, 330–351; b) F. Q. Schafer, G. R. Buettner, *Free Radical Biology and Medicine* **2001**, *30*, 1191–1212; c) S. Dimmeler, A. M. Zeiher, *Cell* **2007**, *130*, 401–402.
- [3] R. L. Krauth-Siegel, H. Bauer, R. H. Schirmer, *Angew. Chem.* **2005**, *117*, 698–724; *Angew. Chem. Int. Ed.* **2005**, *44*, 690–715.
- [4] K. J. Ritchie, S. Walsh, O. J. Sansom, C. J. Henderson, C. R. Wolf, *Proc. Natl. Acad. Sci. USA* **2009**, *106*, 20859–20864.
- [5] G. Wu, Y. Z. Fang, S. Yang, J. R. Lupton, N. D. Turner, *J. Nutr.* **2004**, *134*, 489–492.
- [6] V. B. Djordjević, *Int. Rev. Cytol.* **2004**, *237*, 57–89.
- [7] A. Pompella, A. Visvikis, A. Paolicchi, V. De Tata, A. F. Casini, *Biochem. Pharmacol.* **2003**, *66*, 1499–1503.
- [8] D. B. Smith, K. S. Johnson, *Gene* **1988**, *67*, 31–40.
- [9] a) H.-S. Ro, B. H. Koh, S. O. Jung, H. K. Park, Y.-B. Shin, M.-G. Kim, B. H. Chung, *Proteomics* **2006**, *6*, 2108–2111; b) J.-W. Jung, S.-H. Jung, H.-S. Kim, J. S. Yuk, J.-B. Park, Y.-M. Kim, J.-A. Han, P.-H. Kim, K.-S. Ha, *Proteomics* **2006**, *6*, 1110–1120.
- [10] C. M. Kolodziej, C.-W. Chang, H. D. Maynard, *J. Mater. Chem.* **2011**, *21*, 1457–1461.
- [11] a) A. del Campo, D. Boos, H. W. Spiess, U. Jonas, *Angew. Chem.* **2005**, *117*, 4785–4791; *Angew. Chem. Int. Ed.* **2005**, *44*, 4707–4712; b) J. M. Alonso, A. Reichel, J. Piehler, A. del Campo, *Langmuir* **2008**, *24*, 448–457; c) G. Mayer, A. Heckel, *Angew. Chem.* **2006**, *118*, 5020–5042; *Angew. Chem. Int. Ed.* **2006**, *45*, 4900–4921; d) G. C. R. Ellis-Davies, *Nat. Methods* **2007**, *4*, 619–628; e) M. Goeldner, R. Givens, *Dynamic Studies in Biology*, Wiley-VCH, Weinheim, **2005**.
- [12] M. C. Pirrung, C. Y. Huang, *Bioconjugate Chem.* **1996**, *7*, 317–321.
- [13] S. Banala, A. Arnold, K. Johnsson, *ChemBioChem* **2008**, *9*, 38–41.
- [14] a) C. Grunwald, K. Schulze, A. Reichel, V. U. Weiss, D. Blaas, J. Piehler, K. H. Wiesmüller, R. Tampé, *Proc. Natl. Acad. Sci. USA* **2010**, *107*, 6146–6151; b) M. Bhagawati, S. Lata, R. Tampé, J. Piehler, *J. Am. Chem. Soc.* **2010**, *132*, 5932–5933.
- [15] T. Fehrentz, M. Schönberger, D. Trauner, *Angew. Chem.* **2011**, *123*, 12362–12390; *Angew. Chem. Int. Ed.* **2011**, *50*, 12156–12182.
- [16] a) S. Fodor, J. Read, M. Pirrung, L. Stryer, A. Lu, D. Solas, *Science* **1991**, *251*, 767–773; b) S. Li, D. Bowerman, N. Marthandan, S. Klyza, K. J. Luebke, H. R. Garner, T. Kodadek, *J. Am. Chem. Soc.* **2004**, *126*, 4088–4089.
- [17] a) A. Deiters, *Curr. Opin. Chem. Biol.* **2009**, *13*, 678–686; b) X. Tang, I. J. Dmochowski, *Mol. Biosyst.* **2007**, *3*, 100–110.
- [18] S. Petersen, J. M. Alonso, A. Specht, P. Duodu, M. Goeldner, A. del Campo, *Angew. Chem.* **2008**, *120*, 3236–3239; *Angew. Chem. Int. Ed.* **2008**, *47*, 3192–3195.
- [19] S. Walbert, W. Pfeleiderer, U. E. Steiner, *Helv. Chim. Acta* **2001**, *84*, 1601–1611.
- [20] A. E. Adang, J. Brussee, A. van der Gen, G. J. Mulder, *Biochem. J.* **1990**, *269*, 47–54.
- [21] S. Raghunathan, R. J. Chandross, R. H. Kretsinger, T. J. Allison, C. J. Penington, G. S. Rule, *J. Mol. Biol.* **1994**, *238*, 815–832.
- [22] I. Jakobson, M. Warholm, B. Mannervik, *J. Biol. Chem.* **1979**, *254*, 7085–7089.
- [23] S. F. Martin, M. H. Tatham, R. T. Hay, I. D. W. Samuel, *Protein Sci.* **2008**, *17*, 777–784.
- [24] G. MacBeath, S. L. Schreiber, *Science* **2000**, *289*, 1760–1763.